Molecular Crystals and Liquid Crystals
Publication details, including instructions for authors and subscription information:
http://www.tandfonline.com/loi/gmcl20

# VLSI Photonics: How Can We Approach Using Micro/Nano-Materials?

El-Hang Lee [a] , Hyun-Shik Lee [a] , Yong Ku Kwon [a] , Kyong-Hon Kim [a] , Seung-Gol Lee [a] & Beom-Hoan O [a]

[a] OPERA National Research Center for VLSI Photonics, Micro/nano-Photonics Advanced Research Center (m-PARC), Graduate School of Information Technology, INHA University, Incheon, South Korea

Version of record first published: 28 May 2010

To cite this article: El-Hang Lee, Hyun-Shik Lee, Yong Ku Kwon, Kyong-Hon Kim, Seung-Gol Lee & Beom-Hoan O (2010): VLSI Photonics: How Can We Approach Using Micro/Nano-Materials?, Molecular Crystals and Liquid Crystals, 522:1, 159/[459]-171/[471]

To link to this article: http://dx.doi.org/10.1080/15421401003726899

*Mol. Cryst. Liq. Cryst.*, Vol. 522: pp. 159/[459]–171/[471], 2010

ISSN: 1542-1406 print/1563-5287 online
DOI: 10.1080/15421401003726899



# VLSI Photonics: How Can We Approach Using Micro/Nano-Materials?

EL-HANG LEE, HYUN-SHIK LEE, YONG KU KWON, KYONG-HON KIM, SEUNG-GOL LEE, AND BEOM-HOAN O

OPERA National Research Center for VLSI Photonics, Micro/nano-Photonics Advanced Research Center (m-PARC), Graduate School of Information Technology, INHA University, Incheon, South Korea

*This paper presents our recent results on the materials science and engineering research that we are pursuing for what we call very large scale integrated (VLSI) micro/nano-photonic circuit applications and optical printed circuit board (O-PCB) applications. It discusses on the design and fabrication of optical waveguides and photonic devices to be part of the micro/nano-photonic integration for VLSI photonic integrated circuits of generic and application-specific nature. The optical circuits consist of 2-dimensional planar arrays of micro/nano-optical wires, circuits and devices to perform various functions. The integrated optical circuits are primarily made of polymer and silicon materials. We present the use of organic-inorganic hybrid materials for micro-scale optical waveguide fabrication and discuss various attempts to vary the optical properties such as refractive indices, transmission windows, losses, birefringence, dispersion, nonlinearity, thermal/mechanical stability, and related issues. These waveguides and devices are considered particularly useful for O-PCB fabrication. We then present the use of silicon as a basic material for VLSI photonic devices. We discuss their properties and advantages for nano-scale functional waveguides and devices for VLSI photonics. We will look into the use of silicon materials as the basis for the building blocks of VLSI photonics. We will finally discuss the issues regarding how these building blocks can be put together for integration for O-PCB and VLSI photonic chips.*

**Keywords** Hybrid materials; optical circuit; photonic devices; VLSI photonics



## Introduction

In recent years, we have proposed the concept of optical printed circuit board (O-PCB) and the concept of very large scale integrated (VLSI) photonics as new means of achieving micro/nano-scale integration of increasing number of photonic building blocks such as nano-wires, photonic crystal devices, micro-ring devices,

Address correspondence to El-Hang Lee, OPERA National Research Center for VLSI Photonics, Micro/nano-Photonics Advanced Research Center (m-PARC), Graduate School of Information Technology, INHA University, Incheon 402-751, Republic of Korea. E-mail: ehlee@inha.ac.kr

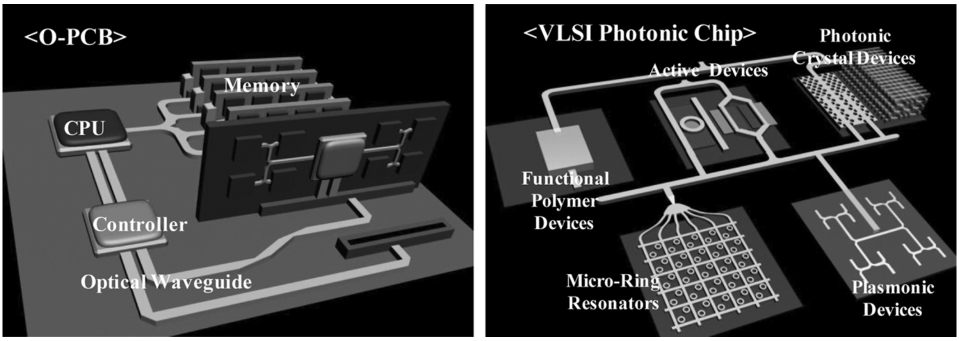


**Figure 1.** Schematic diagram of O-PCB and VLSI photonic chip.



plasmonic devices, and others. O-PCB consists of optical waveguides made of polymer materials in arrays to interconnect and integrate micro/nano-scale photonic circuits and devices on a planar board, either rigid or flexible. VLSI photonic circuits consist of integrated nano-scale wires and devices in high densities [1–3]. Figure 1 shows the schematic diagrams of the O-PCB and the VLSI photonic chips.

Conceptually, the O-PCBs and VLSI-photonic integrated circuits (IC) process optical signals through optical wires as opposed to the traditional E-PCBs and VLSI-electronic ICs which process electrical signals through electrical wires. The VLSI micro/nano-photonic integrated systems are to be compact, intelligent, high-speed, light-weight, environmentally friendly, low-powered, and low-cost as applicable for datacom, telecom, transportation, aero-space, avionics, bio/medical, sensor, and environmental systems and are designed to integrate functional micro/nano-devices and circuits of information technology (IT), bio-technology (BT) and nano-technology (NT) for broad based applications and usages. The new optical circuits are to consist of 2-dimensional planar arrays of micro/nano-optical wires, circuits and devices to perform the functions of sensing, storing, transporting, processing, switching, routing and distributing optical signals. The integrated optical components include micro/nano-scale light sources, waveguides, detectors, switches, modulators, sensors, directional couplers, multi-mode interference devices, wavelength filters, micro-ring resonator devices, photonic crystal devices, plasmonic devices, and quantum devices, made of polymer, silicon and other semiconductor materials.

We discuss some of the technological issues and challenges of achieving O-PCBs and VLSI photonic circuits and present our recent progresses regarding the use of polymer materials and silicon materials for O-PCB fabrication and VLSI photonic circuit fabrication. In general, the issues should include those of miniaturization and integration of micro/nano-scale photonic materials, devices, and circuits leading to ultra-small and very large scale integration. They should include the compatibility issues between micro/nano-devices such as materials mismatch, size mismatch, mode mismatch, optical mismatch, mechanical/thermal mismatch and the nano-optical effects such as micro-cavity effects, non-linear effects, and quantum optical effects in nano-scale devices. In this paper, we will focus on the basic materials requirements of the micro/nano-wires and devices to be used for O-PCB and VLSI photonics. These include optical refractive indices, transmission windows, losses, birefringence, dispersion, nonlinearity, thermal/mechanical stability, and others. Primarily, polymer materials or the organic-inorganic hybrid materials have been used for

O-PCB fabrication and silicon materials are used for VLSI photonic application. We will present some examples of building block photonic devices such as polymer waveguides, silicon waveguides, micro-ring devices, non-linear devices, and plasmonic waveguides that have been designed and fabricated for integration on the O-PCB and VLSI photonic chips.

## Organic-Inorganic Hybrid Materials

Inorganic materials are widely used for modern integrated optics due to their excellent thermal stability, chemical inertness, transparency and low birefringence [4–11]. However, these materials have the disadvantage of a high production cost compared with other materials. On the other hand, polymeric materials contain hydrocarbon units, which experience a large transmission loss in the near-infrared red region due to the vibrational overtone absorption of the aliphatic chains [12–14]. In an attempt to reduce the optical loss of these hydrocarbon polymers, deuterated or halogenated polymers have been prepared. Various optical polymers have been commercialized, but the high cost of producing these compounds limits their extensive use in photonics [15–22]. In addition, polymeric materials experience a large volume shrinkage induced by curing as well as internal stress during many fabrication processes, resulting in an increase in the level of optical loss at key communication wavelengths. In order to achieve material properties, superior to single organic or inorganic components, various types of composite materials in which two different phases with complementary physical properties are combined, have been introduced. Recently, new types of organic-inorganic hybrid materials have been developed and studied as waveguide materials [23–31]. Unlike classical approaches to produce macroscopic composite materials simply by mixing inorganic materials with organic

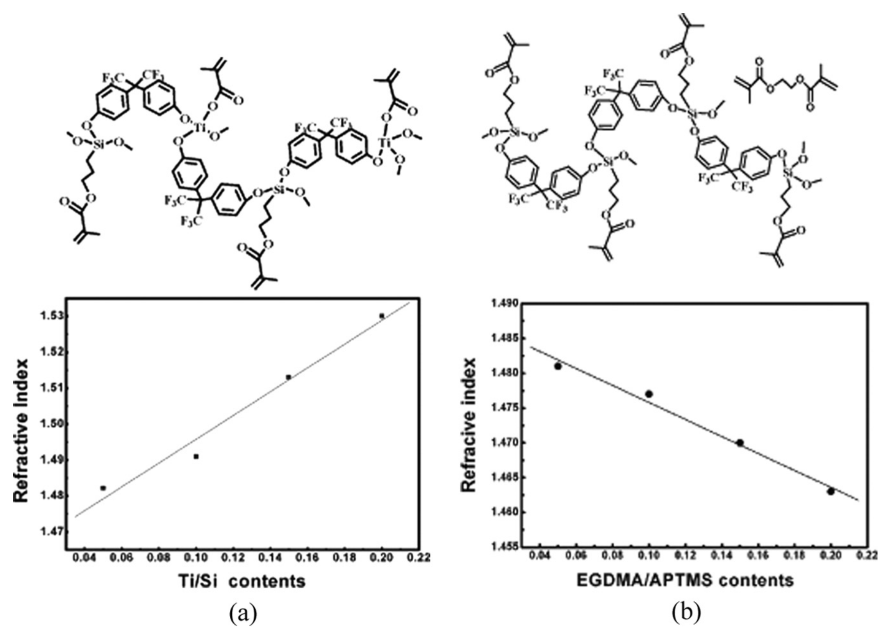


**Figure 2.** Change in the measured in-plane refractive index as a function of chemical composition.

compounds, they are prepared by sol-gel processing. Using this method, an organic-inorganic network-like structure is formed by crosslinking through a polycondensation reaction between inorganic precursors and organic compounds.

Recently we have synthesized a series of organic-inorganic hybrid materials by a non-hydrolytic sol-gel reaction [31]. Adjusting the chemical composition of the materials allows the precise tailoring of the optical properties of the materials, such as optical loss, birefringence, refractive index, and thermo-optic coefficient. In particular, the tunability of the refractive index allows the fabrication of the step-index optical waveguide structure with well-defined and reproducible refractive index differences to within 0.0001. This method avoids high volume shrinkage during further treatment of the films and is therefore suitable for soft molding processes. Here we prepared a series of organic-inorganic hybrid materials of titanium methacrylate triisopropoxide or 3-(acryloxypropyl)trimethoxysilane and 4,4′-(hexafluoroisopropylidene)diphenol and demonstrated the change of the measured refractive index as a function of the chemical composition of the materials (Fig. 2).

## Hybrid Materials for O-PCB Waveguide Fabrication

### *Imprinting*

Hybrid materials are among the most promising candidates for use in photonics due to their versatility, flexibility, light weight, low cost and ease of modification [23–31]. These materials are relatively easy to produce and suitable for the formation of a large area. A series of optical waveguides using these organic-inorganic hybrid materials can be fabricated by exploiting a soft lithography technique. Unlike conventional lithography such as photoresist-based patterning, the soft lithography technique is more effective for the fabrication of microstructures as they typically can be carried out at a low cost without the need for large-scale facilities.

### *Imprinting by PDMS Mold*

For the preparation of a multimode ridge waveguide, imprinting techniques or embossing techniques were employed. Figure 3 shows a schematic representation of the preparation of optical waveguide from organic-inorganic hybrid materials by soft lithographic technique. In this process, the undercladding material with low refractive index is first spin-coated onto the substrate and is then cured by photo-polymerization. Then, the core material with slightly high refractive index is

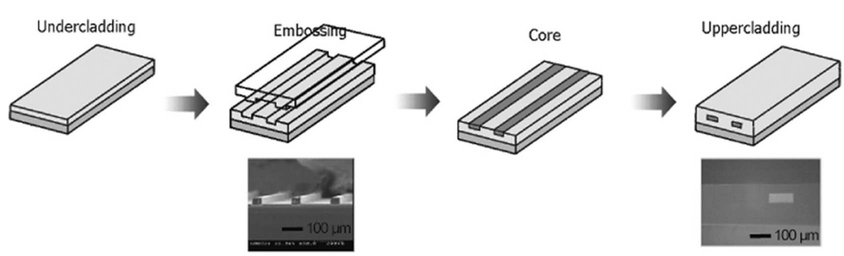


**Figure 3.** Schematic representation of the preparation of optical waveguide from organic-inorganic hybrid materials by soft lithographic technique.

coated onto the undercladding layer and a polydimethylsiloxane (PDMS) mold is pressed onto it. In our study, after removing the air between the mold and the film, the PDMS mold and the films were exposed to ultraviolet (UV) light for photo-polymerization. After removing the PDMS mold, the uppercladding material which was the same as the undercladding material was coated both onto the core and the undercladding, and a flat glass was again pressed onto them. After a UV exposure and a heat-treatment of 150°C, a multimode optical waveguide was successfully prepared. We found the surfaces of these hybrid films flat and smooth. It was also found that these films contain no cracks and their thickness on the substrate was uniform.

### *Silicon Mold for Imprinting*

Waveguides can also be imprinted using silicon mold. Imprinting is done by utilizing a patterned mold pressed into a resin for structure definition and it is emerging as a fast low-cost and high-volume production. The imprinting is done by either thermal or ultraviolet (UV) imprinting techniques using a silicon mold.

We fabricated silicon molds by wet chemical etching. First, a 1um-thick $SiO_2$ layer was thermally grown on a silicon substrate and was patterned with photolithography technique. The patterned silicon substrate was etched with a buffered oxide etchant (BOE) solution to transfer the photoresist patterns to the $SiO_2$ layer. The patterned silicon substrate was then immersed in a 15 M KOH solution at 75°C to get 50 um-high vertically etched rectangular structures and the remaining $SiO_2$ mask film is removed. The silicon waveguide mold was then completed.

An anti-sticking layer on the silicon mold is essential to both UV and thermal imprinting techniques. There are two conventional methods to form an anti-sticking layer: Teflon-like film coating and self-assembled monolayer (SAM) coating. We used SAM coating because the SAM coating can form a uniform anti-sticking layer on the sidewall of the silicon mold. For the SAM coating the silicon mold is first soaked in a diclorodimethylsilane (DDMS) based solution for 1 hour. Then, we obtained a completed silicon mold coated with an anti-sticking layer.

### *Thermal Imprinting of Optical Wires with Silicon Mold*

We fabricated an array of twelve channel embedded waveguides by thermal imprinting technique. For thermal imprinting we used polymethylmethacrylate (PMMA) sheet of 400 micron thickness as cladding material. The refractive index of the PMMA sheet is 1.49 at 850 nm wavelength. First, we molded the PMMA under-cladding layer by using the silicon mold. We thermally heated it to 170°C, and pressed it at 20 bar for 2 min. The UV curable polymer having an index of 1.51 was dropped on the molded under-cladding layer and was covered with a transparent glass wafer. This optical layer was then pressed at 10 bar and was irradiated by a UV source. After the glass wafer was detached, another UV-curable polymer layer with the index of 1.45 at 850 nm wavelength was coated on the replicated waveguide array as an upper-cladding layer. The cross-sectional dimension of the fabricated waveguide arrays was 50 microns in width, 50 microns in height, and 7 cm in length. The waveguides were formed at a pitch of 250 microns to match the size of the ribbon fiber cable.

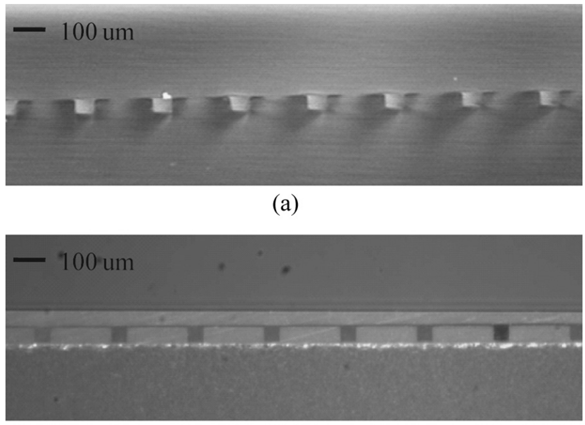


(b)

**Figure 4.** Cross-sectional views of fabricated optical waveguides (a) by hot imprinting technique and (b) by UV imprinting technique.



### *UV Imprinting of Optical Wires with Silicon Mold*

First, we dropped a UV-curable polymer of refractive index of 1.450 at 850 nm wavelength on a glass substrate. The under-cladding layer was imprinted with a silicon mold and was irradiated with UV at 7 bar pressure for 2 min. Another UV curable polymer with refractive index of 1.470 at 850 nm wavelength was dropped over the embossed under-cladding layer and was covered with upper-cladding polymer layer. This entire optical layer was the pressed at 7 bar, and was irradiated with a UV source.

## Silicon Materials for Micro/Nano-Photonic Devices

### *Silicon Device Fabrication*

One of the advantages of using silicon for photonic devices is the fact that silicon is basically transparent at the optical communication wavelength. Another advantage of using silicon for photonic devices is that silicon has a high refractive index at these wavelengths, which can allow high confinement effect of the lightwaves.

Silicon optical devices are fabricated on silicon-on-insulator (SOI) wafers. SOI wafers have a thin crystalline top silicon layer which is separated from the underlying silicon wafer by an intermediate thin layer of oxide formed in-between. Especially on SOI, silicon-based nano-scale photonic devices can benefit much from the high refractive index contrast between the silicon and the $SiO_2$ (3.48 – 1.46 at 1.55um wavelength). SOI-based photonic devices therefore have much room to be miniaturized to small devices due to the high refractive index contrast and high light confinement effect. The optical mode of the silicon waveguide, when surrounded by air or $SiO_{2,}$ can be confined to subwavelength dimension, typically several hundred nanometers width and height. This not only provides a way to achieve very high density optical wiring on VLSI photonic chips but also offers feasible solutions to achieve integration of photonic devices and electronic devices in a manner that is compatible with the conventional silicon manufacturing process.

The overall fabrication process of the silicon nano-photonic devices is compatible with that of the 0.18 um complementary metal-oxide semiconductor (CMOS) process.

However, some devices require a tighter critical dimension (CD) control below 100 nm scale and such devices include the inverse taper structure, fine pitch one-dimensional (1-D) photonic crystal for Bragg reflector, and two-dimensional (2-D) photonic crystals used as a cavity structure [32–35]. These structures need a special care when the optical lithography process is used for pattern definition. Electron beam lithography can create sub-10 nm scale features and, therefore, it is an ideal tool for nano-scale patterning in spite of its slow writing speed. In the case of the dry etching process, it is also important to control the sidewall roughness of the etched patterns so as to minimize scattering loss of the waveguide device. The etched profile and roughness of the structure is a complex result from the mask material, mask sidewall roughness, etching gas mixture, chemistry, and pattern design itself. The post-etch treatment such as thermal oxidation, wet etching, and plasma treatment can be used to reduce the sidewall roughness. However, these processes consume some amount of silicon layer which might affect the device performance.

In our study we used Electron Beam Lithography (EBL) and the Nano-Imprint Lithography (NIC) techniques for the fabrication of the silicon waveguides and devices. In the EBL process, we prepared a SOI wafer and coated the 350 nm electron-beam (EB) resist of polymethylmethacrylate (PMMA) on a silicon wafer and patterned it using EBL at an acceleration voltage of 100 KeV. We etched the patterned silicon wafer using inductive coupled plasma reactive ion etcher (ICP-RIE). The $SF_6$, Ar and $Cl_2$ mixture etching gas was used for achieving the vertical etched sidewall slope. The etching time was 2 min and after etching we cleaned the residual EB resist using $O_2$ asher. We could obtain high resolution silicon optical waveguides. As the propagation loss of a single mode in a highly confined silicon waveguide depends greatly on the surface roughness, the surface roughness should be minimized as much as possible during the process of fabrication. Further, in order to increase the integration density of silicon optical wires and devices, special attention has to be paid to the control of the roughness of the etched surfaces of the silicon.

Compared to EBL and deep ultraviolet Lithography (DUVL) techniques, NIL utilizes a patterned template that is pressed into a resist for structure definition, and it is emerging as a fast low-cost and high-volume production method [36–42]. Normally in the ultraviolet nanoimprint lithography (UV-NIL) a UV-transparent mold is used when the substrate is opaque like silicon. Especially in our study we proposed the use of ultraviolet (UV) transparent polymer molds for UV-nanoimprint lithography (UV-NIL) for nano-photonic devices and circuits. The advantages of the UV-transparent polymer mold are to allow their use for opaque substrates like silicon and to reduce the residual layer. The absence of a high pressure results in a near-zero residual layer, which is a significant advantage.

In the NIL process using polymer mold, we fabricated the silicon master using EBL as described above. In the NIL process one of the most important factors is to smoothly detach the mold from the replica. As silicon is sticky to polymer materials, a treatment is needed to prevent the sticking problem during the polymer mold replication. We thus coated an anti-adhesion layer of dimethyldichlorosilane (DDMS) on the surface of the silicon master using self assembled monolayer (SAM). The polymer mold is then easily detached from the silicon master. We dropped the UV resin on a glass substrate and imprint it with the silicon master. Here, we used a low viscosity UV curable resin for nano-scale pattering. It was pressed at 20 bar and was exposed to UV radiation for 15 seconds.

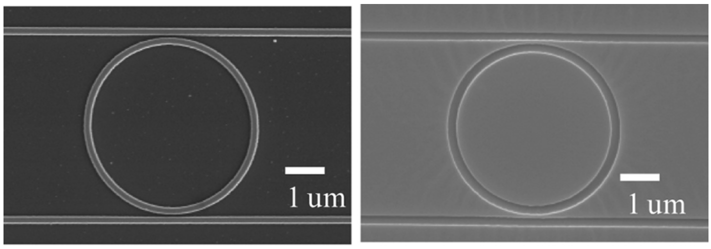


(a) (b)

**Figure 5.** SEM images of the micro-ring resonator made of (a) silicon and (b) polymer on SOI wafer.



Using this mold we were able to pattern the resist on the SOI wafer and fabricate photonic devices by silicon dry-etching. We spin-coated the UV resin on the SOI wafer and imprinted it with the polymer mold. The thickness of the UV resin was about 2 μm. It was exposed to UV radiation for 15 seconds at a pressure of 50 bar. We obtained the residual thickness less than 5 nm. Since the residual layer makes it difficult to obtain the vertical etched sidewall we removed the residual layer using $O_2$ asher for 1 min. We obtained the resist pattern on SOI wafer with zero residual layer and etched it to get the silicon photonic device patterns by the ICP-RIE technique. For practical application, we also fabricated nanowire ring resonators. Figure 5 shows the scanning electron microscope (SEM) images of the nanowire ring resonator. The dimension of the silicon nanowire is 300 nm wide and 200 nm high. The radius of the ring resonator is about 5 μm and the separation distance between two nanowires is 100 nm.

### *Silicon Nonlinear Nano-Photonic Devices with Polymer Clad*

In recent years, as mentioned above, silicon materials have been studied by many research groups for potential application to nonlinear nanophotonic devices because of high refractive index properties of the silicon [43–47]. Large refractive index difference between the core silicon and $SiO_2$ or polymer material clad, as mentioned above, allows very small cross-sectional size of the single-mode silicon waveguides in a submicron scale and a tight optical confinement to enhance the nonlinear optical properties. With these positive properties of the silicon waveguide the length of the nonlinear functional silicon devices can be made very short in an order of millimeter scale. However, there have been several reports that the phase matching condition between a pump beam and nonlinear effect-induced optical beams is very important for efficient four-wave-mixing (FWM) based nonlinear optical devices [48–50]. Foster *et al.* have reported that anomalous group-velocity dispersion (GVD) condition of the pump beam wavelength is required in the silicon core waveguides to achieve the phase matching condition between the pump and FWM-generated signals [43].

We have performed numerically analysis for the tailored anomalous GVD condition of the silicon waveguides with a polymer clad on SOI wafer. We consider the silicon strip waveguides formed on a $SiO_2$ layer of the SOI wafer with an over-coated polymer clad which are relatively easy schemes for device fabrication as well as dispersion control compared to the buried silicon core in its $SiO_2$ layer as reported in the previous studies by Turner *et al.* [51]. and Yin *et al.* [52]. Figure 6 shows

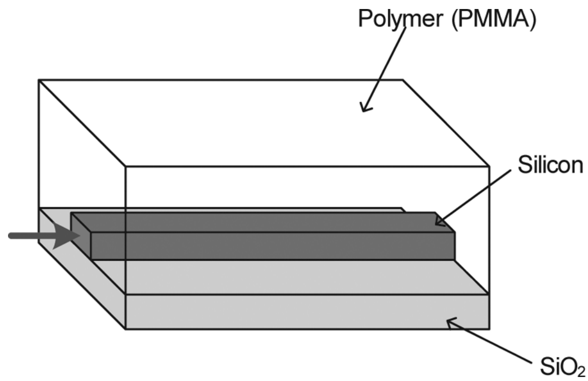


**Figure 6.** A silicon waveguide scheme with a polymer cladding.



the strip-channel-type silicon waveguide scheme with a polymer clad considered for our numerical analysis. A proper choice of the polymer clad material allows the control of the chromatic dispersion properties of the silicon waveguides formed on a $SiO_2$ layer. A commercial finite element method software is used to find the wave propagation constant $\beta$ along the silicon waveguides for a given waveguide structure at a specific wavelength, and then to calculate the effective index of refractions $n_{\mathrm{eff}}$ for the silicon waveguides from $n_{\mathrm{eff}} = \beta/k$. $k = 2\pi/\lambda$ is the free-space wave propagation constant for the wavelength $\lambda$. Then, the GVD of the waveguide $D$ can be obtained from

$$D = -\frac{\lambda}{c}\frac{d^2 n_{\mathrm{eff}}}{d\lambda^2} \tag{1}$$

Numerically calculated results on the GVD of the silicon waveguide with a PMMA polymer cladding for the wavelength of 1550 nm are shown in Figure 7. Figure 7(a) and (b) show the calculated GVDs for various waveguide widths at a fixed waveguide height of 300 nm and for various waveguide heights at a fixed waveguide width of 400 nm, respectively. In this numerical analysis, the Sellmeier formulae and coefficients for the silicon, $SiO_2$ and PMMA taken from references [48,51,52], are used. The GVD values of the waveguides become anomalous as the waveguide width becomes greater than 350 nm for the fixed waveguide height of 300 nm or as the waveguide height becomes higher than 250 nm at the fixed waveguide width of 400 nm. In this calculation the PMMA polymer cladding case was considered. In order to have high nonlinear property of the silicon waveguide, its waveguide size should be as small as possible, but should not be too small to guarantee a low optical loss of light beam propagation.

## Optical Characterization of Waveguides and Materials

An optical low coherence reflectometer was developed for measuring the propagation loss and any internal defects of the optical wire embedded in an O-PCB and its schematic diagram is shown in Figure 8. The balanced detection scheme was used to increase the signal-to-noise ratio of the measuring system [53,54]. By changing the optical path length of the reference arm and using a low-coherence light source, the reference beam can be selectively interfered with a signal beam reflected

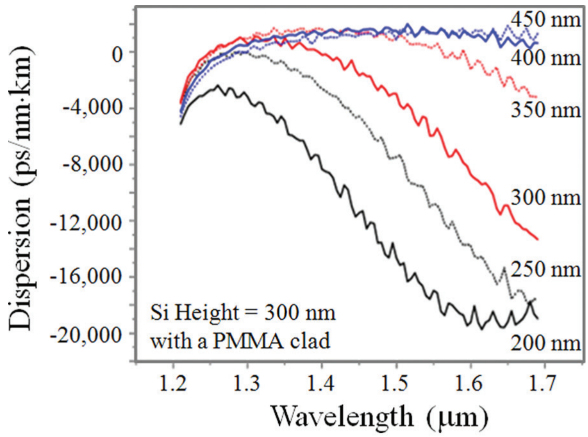


(a)

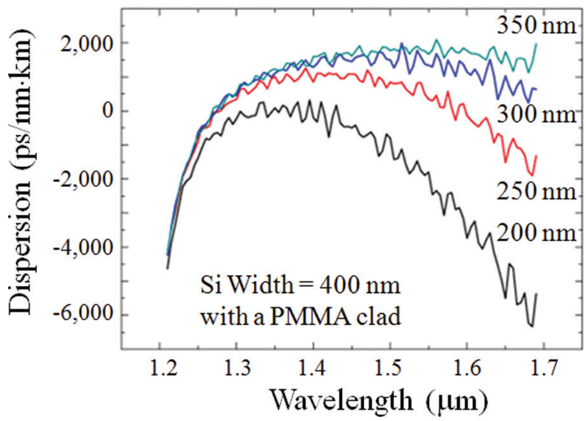


(b)

**Figure 7.** Numerically calculated chromatic dispersion of the silicon waveguide with a polymer cladding (a) for various waveguide widths at a fixed waveguide height of 300 nm and (b) for various waveguide heights at a fixed waveguide width of 400 nm.

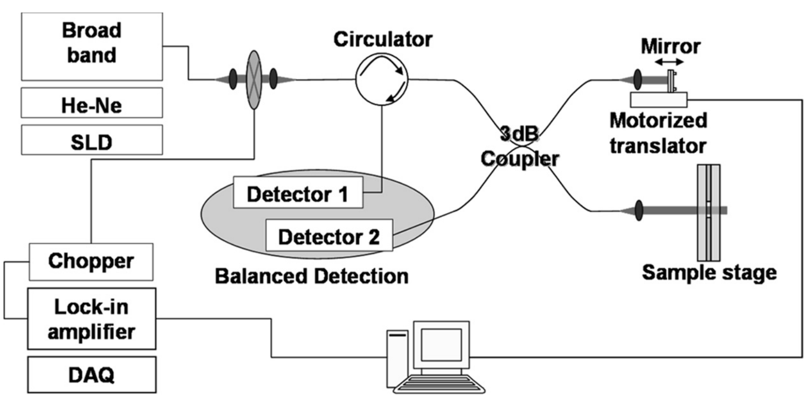


**Figure 8.** Schematic diagram of an optical low coherence reflectometer for measuring the propagation loss and any internal defects of the optical wire embedded in an O-PCB.

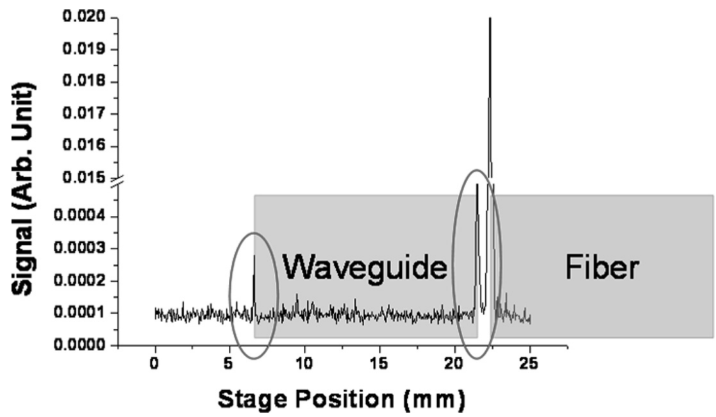


**Figure 9.** The variation of the interference signal according to movement of the mirror placed at the reference arm.



from any internal cross-section of the optical wire. The optical path length of the reference beam was controlled by moving the mirror mounted on motorized translator.

A short waveguide coupled to the end of an optical fiber was measured with the reflectometer, and the measured interferogram is shown in Figure 9. The locations of the input and output ends of the optical wire can be found from two interference peaks in the figure. In addition, the propagation loss of the optical wire can be estimated from the intensity ratio of the same interference peaks.

## Interconnection and Integration

Integration in photonics is one of the most important issues for achieving VLSI photonic circuits. For integration and interconnection, various issues such as mode mismatch, size mismatch and index mismatch should be considered. Further, in nano-scale photonic interconnection, issues such as non-linear effects must be taken into account. Generally the non-linear parameters are inversely proportional to the effective cross-section of the optical waveguides [55]. Hence, the non-linear parameters such as self phase modulation and cross phase modulation, parametric gain in four wave mixing, and effective Raman gain in simulated Raman scattering, are taken into consideration for the nanophotonic interconnection and integration.

We investigated the issues of the integration between, for example, a silicon waveguide and a surface plasmon polaritons (SPP) waveguide. The SPP waveguide is a promising candidate to achieve nano-scale photonic integrated circuits because the modal size of the SPP can be reduced much below the wavelength [56–58]. However, the large propagation loss in the SPP waveguide may limit the use of SPP waveguide for long range signal transmission. Hence, integration between a SPP waveguide and a silicon waveguide can become a solution to circumvent the problem of the propagation loss of the SPP waveguide. We investigated on the issues of integrating a SPP waveguide and a silicon waveguide in terms of optical impedance matching and polarization matching. A guided wave coupler was used for achieving the optical impedance matching and polarization matching in the integration of these waveguides [59]. These results will be presented in future publications.

## Acknowledgments

This work has been supported by the Korea Science and Engineering Foundation (KOSEF) of the Ministry of Education and Science (MES) through the grant for the National Research Center for VLSI Photonic Integration (R11-2003-022) at the Optics and Photonics Elite Research Academy (OPERA), Inha University, Incheon, South Korea.

## References

[1] Lee, E. H., Lee, S. G., O, B. H., & Park, S. G. (2004). *IEEE LEOS Newsletters*, *18*, 15.
[2] Lee, E.-H., Lee, S.-G., O, B. H., Jeong, M.-Y., Kim, K.-H., & Song, S.-H. (2006). *Microelectronic Engineering*, *83*, 1767.
[3] Lee, H. S., An, S.-M., Kim, Y., Kim, D.-G., Kang, J.-K., Choi, Y.-W., Lee, S.-G., O, B. H., & Lee, E.-H. (2006). *Microelectronic Engineering*, *83*, 1347.
[4] Miya, T. (2000). *IEEE J. Select. Top. Quant. Electron.*, *6*, 38.
[5] Lai, Q., Bachmann, M., & Melchior, H. (1997). *Electron Lett.*, *33*, 1699.
[6] Worhoff, K., Lambeck, P. V., & Driessen, A. (1999). *J. Lightwave Technol.*, *17*, 1401.
[7] Roussev, R. V., Langrock, C., Kurz, J. R., Fejer, M. M. (2004). *Opt. Lett.*, *29*, 1518.
[8] Hu, H., Lu, F., Chen, F., Shi, B. R., Wang, K. M., & Shen, D. Y. (2001). *J. Appl. Phys.*, *89*, 5224.
[9] Soole, J. B. D., Amersfoort, M. R., LeBlanc, H. P., Andreadakis, N. C., Rajhel, A., Caneau, C., Koza, M. A., Bhat, R., Youtsey, C., & Adesida, I. (1996). *Electron. Lett.*, *32*, 323.
[10] Bissessur, H., Gaborit, F., Martin, B., Ripoche, G., & Pagnodrossiaux, P. (1995). *Electron. Lett.*, *31*, 32.
[11] Ooi, B. S., McIlvaney, K., Street, M. W., Helmy, A. S., Ayling, S. G., Bryce, A. C., Marsh, J. H., & Roberts, J. S. (1997). *IEEE J. Quant. Electron.*, *33*, 1784.
[12] Eldada, L. (2004). *Rev. Sci. Instrum.*, *75*, 575.
[13] Eldada, L. & Shacklette, L. W. (2000). *IEEE J. Select. Top. Quant. Electron.*, *6*, 54.
[14] Ma, H., Jen, A. K.-Y., & Dalton, L. D. (2002). *Adv. Mater.*, *14*, 1339.
[15] Booth, B. L. (1989). *J. Lightwave Technol.*, *7*, 1445.
[16] Yoshimura, R., Hikita, M., Tomaru, S., & Imamura, S. (1998). *J. Lightwave Technol.*, *16*, 1030.
[17] Imamura, S., Yoshimura, R. & Izawa, T. (1991). *Electron. Lett.*, *27*, 1342.
[18] Kobayashi, J., Matsuura, T., Hida, Y., Sasaki, S., & Maruno, T. (1998). *J. Lightwave Technol.*, *16*, 1024.
[19] Kobayashi, J., Matsuura, T., Hida, Y., Sasaki, S., & Maruno, T. (1998). *Appl. Opt.*, *37*, 1032.
[20] Babb, D. A., Ezzell, B. R., Clement, K. S., Richey, W. F., & Kennedy, A. P. (1993). *J. Polym. Sci. Polym. Chem.*, *31*, 3465.
[21] Reyes, G. D. L., Quema, A., Ponseca, C., Pobre, R., Quiroga, R., Ono, S., Murakami, H., Estacio, E., Sarukura, N., Aosaki, K., Sakane, Y., & Sato, H. (2006). *Appl. Phys. Lett.*, *89*, 2111.
[22] Lowry, J. H., Mendlowitz, J. S., & Subramanian, N. S. (1992). *Opt. Eng.*, *31*, 1982.
[23] Brinker, C. J. & Scherer, G. W. (1990). *Sol-Gel Science*, Academic Press: Boston.
[24] Xu, C., Eldada, L., Wu, C., Norwood, R. A., Shacklette, L. W., Yardley, J. T., & Wei, Y. (1996). *Chem. Mater.*, *8*, 2701.
[25] Motakef, S., Boulton, J. M., & Uhlmann, D. R. (1994). *Opt. Lett.*, *19*, 1125.
[26] Krug, H., Merl, N., & Schmidt, H. (1992). *J. Non-Cryst. Solids*, *147*, 447.
[27] Yoshida, M. & Prasad, P. N. (1996). *Chem. Mater.*, *8*, 235.
[28] Lee, K. S., Wung, C. J., Prasad, P. N., Kim, C., Park, C. K., Jim, J. I., & Shim, H. K. (1993). *Mol. Cryst. Liq. Cryst.*, *224*, 33.
[29] Jung, J. I., Park, O. H., & Bae, B. S. (2003). *J. Sol-Gel Sci. Tech.*, *26*, 897.

[30] Yoldas, B. E. (1986). *J. Mater. Sci.*, *21*, 1087.
[31] Kwon, Y. K., Han, J. K., Lee, J. M., Oh, J. H., Lee, H.-S., Lee, E.-H. (2008). *J. Mater. Chem.*, *18*, 579.
[32] Song, B.-S., Noda, S., Asano, T., & Akahane, Y. (2005). *Nature Materials*, *4*, 207.
[33] Tsuchizawa, T., Yamada, K., Fukuda, H., Watanabe, T., Takahashi, J., Takahashi, M., Shoji, T., Tamechika, E., Itabashi, S., & Morita, H. (2005). *Journal of Sel. Topics in Quan. Electro.*, *11*, 232.
[34] Bogaerts, W., Baets, R., Dumon, P., Wiaux, V., Beckx, S., Taillaert, D., Luyssaert, B., Van Campenhout, J., Bienstman, P., & Van Thourhout, D. (2005). *Journal of Lightwave Technol.*, *23*, 401.
[35] Lee, J.-M., Kim, D.-J., Ahn, H., Park, S.-H., & Kim, G. (2008). *Journal of Lightwave Technol.*, *25*, 2236.
[36] Chou, S. Y., Krauss, P. R., & Renstrom, P. J. (1995). *Appl. Phys. Lett.*, *67*, 3114.
[37] Chou, S. Y., Krauss, P. R., & Renstrom, P. J. (1996). *J. Vac. Sci. Technol. B*, *14*, 4129.
[38] Haisma, J., Verheijen, M., & Heuvel, K. (1996). *J. Vac. Sci. Technol. B*, *14*, 4129.
[39] Bender, M., Otto, M., Hadam, B., Spangenberg, B., & Kurz, H. (2002). *Microelectron. Eng.*, *61–62*, 407.
[40] Austin, M. D., Ge, H., Wu, W., Li, M., Yu, Z., Wasserman, D., Lyon, S.A., & Chou, S.Y. (2004). *Appl. Phys. Lett.*, *84*, 5299.
[41] Colburn, M., Johnson, S., Stewart, M., Damle, S., Bailey, T., Choi, B., Wedlake, M., Michaelson, T., Sreenivasan, S. V., Ekerdt, J., & Wilson, C. G. (1999). *Proc. SPIE*, *3676*, 379.
[42] Sreenivasan, S. V., Willson, C. G., Schumaker, N. E., Resnick, D. J. (2002). *Proc. SPIE*, *4688*, 903.
[43] Foster, M. A., Turner, A. C., Sharping, J. E., Schmidt, B. S., Lipson, M., & Gaeta, A. L. (2006). *Nature*, *441*, 960.
[44] Koos, C., Vorreau, P., Vallaitis, T., Dumon, P., Bogaerts, W., Baets, R., Esembeson, B., Biaggio, I., Michinobu, T., Diederich, F., Freude, W., & Leuthold, J. (2009). *Nature Photonics*, *3*, 216.
[45] Espinola, R. L., Dadap, J. I., Osgood, R. M. Jr., McNab, S. J., & Vlasov, Y. A. (2005). *Opt. Express*, *13*, 4341.
[46] Fukuda, H., Yamada, K., Shoji, T., Takahashi, M., Tsuchizawa, T., Watanebe, T., Takahashi, J.-I., & Itabashi, S. I. (2005). *Opt. Express*, *13*, 4629.
[47] Sharping, J. E., Lee, K. F., Foster, M. A., Turner, A. C., Schmidt, B. S., Lipson, M., Gaeta, A. L., & Kumar, P. (2006). *Opt. Express*, *14*, 12388.
[48] Dimitropoulos, D., Raghunathan, V., Claps, R., & Jalali, B. (2004). *Opt. Express*, *12*, 149.
[49] Turner, A. C., Manolatou, C., Schmidt, B. S., Lipson, M., Foster, M. A., Sharping, J. E., & Gaeta, A. L. (2006). *Opt. Express*, *14*, 4357.
[50] Yin, L., Lin, Q., & Agrawal, A. O. (2006). *Opt. Lett.*, *31*, 1295.
[51] Okamoto, K. (2000). *Fundamentals of Optical Waveguides*, Academic Press: New York.
[52] El Rhaleb, H., Celial, N., Roger, J. P., Fournier, D., Boccara, A. C., Zuber, A. (1996). *Thin Solid Films*, *288*, 125.
[53] Canavesi, C., Morichetti, F., Canciamilla, A., Persia, F., & Melloni, A. (2009). *J. Lightwave Tech.*, *27*, 3062.
[54] Cao, D., Yan, M., McGinnis, B., Ticknor, T., Lam, J., Chen, W., Chen, Y. (2002). *Proc. SPIE*, *4805*, 61.
[55] Agrwal, G. P. (2001). *Nonlinear Fiber Optics*, Springer: Berlin.
[56] Betzig, E., Trautman, J. K., Harris, T. D., Weiner, J. S., & Kostelak, R. L. (1991). *Science*, *251*, 1468.
[57] Barnes, W. L., Dereux, A., Ebbesen, T. W. (2003). *Nature*, *424*, 824.
[58] Bozhevolnyi, S. I., Volkov, V. S., Devaux, E., Laluet, J.-Y., & Ebbesen, T. W. (2006). *Nature*, *440*, 508.
[59] Lee, Hyun-Shik & Lee, El-Hang. Unpublished works.